Contents lists available at ScienceDirect

Nuclear Engineering and Technology

journal homepage: www.elsevier.com/locate/net

Original article

Calculation of kinetic parameters β_{eff} and Λ with modified open source Monte Carlo code OpenMC(TD)

J. Romero-Barrientos [a, b, *], J.I. Márquez Damián [c], F. Molina [a, e], M. Zambra [a, f], P. Aguilera [a, d], F. López-Usquiano [a, b], B. Parra [g], A. Ruiz [a, d]

[a] Comisión Chilena de Energía Nuclear, Nueva Bilbao, 12501, Las Condes, Santiago, Chile
[b] Departamento de Física, Facultad de Ciencias Físicas y Matemáticas, Universidad de Chile, Blanco Encalada, 2008, Santiago, Chile
[c] Spallation Physics Group, European Spallation Source ERIC, P.O. Box 176, 22100, Lund, Sweden
[d] Facultad de Ciencias, Departamento de Física, Universidad de Chile, Las Palmeras, 425, Ñuñoa, Santiago, Chile
[e] Departamento de Ciencias Físicas, Universidad Andres Bello, Sazié 2212, 837-0136, Santiago, Chile
[f] Universidad Diego Portales, Manuel Rodríguez Sur 415, Santiago, Chile
[g] Instituto de Física Corpuscular, Parque Científico, C/Catedrático José Beltrán, 2, E-46980, Paterna, Spain

ARTICLE INFO

ABSTRACT

This work presents the methodology used to expand the capabilities of the Monte Carlo code OpenMC for the calculation of reactor kinetic parameters: effective delayed neutron fraction β_{eff} and neutron generation time Λ. The modified code, OpenMC(Time-Dependent) or OpenMC(TD), was then used to calculate the effective delayed neutron fraction by using the prompt method, while the neutron generation time was estimated using the pulsed method, fitting Λ to the decay of the neutron population. OpenMC(TD) is intended to serve as an alternative for the estimation of kinetic parameters when licensed codes are not available. The results obtained are compared to experimental data and MCNP calculated values for 18 benchmark configurations.

© 2021 Korean Nuclear Society, Published by Elsevier Korea LLC. This is an open access article under the CC BY-NC-ND license (http://creativecommons.org/licenses/by-nc-nd/4.0/).

1. Introduction

The determination of the effective delayed neutron fraction β_{eff}, and the mean neutron generation time Λ, play a key role in reactor kinetics. β_{eff} and Λ values indicate the safe reactor operation limits for a given fuel, and the prompt neutron lifetime depending on the fuel burnup, respectively. The estimation of these quantities requires calculating the adjoint neutron flux or taking into account the system time-dependence. One way to achieve the former is by using Monte Carlo transport code MCNP [1], while the latter requires the time monitoring of neutron population. There has been several efforts to include time dependence for transient analysis in Monte Carlo codes such as McCARD [2], Serpent [3], MCNP [4], and added capabilities to OpenMC [5]. In this work the open source

Monte Carlo code OpenMC [6] was modified to explicitly include time-dependency, so kinetic parameters can be estimated. The modified code was named Time-Dependent OpenMC or OpenMC(TD). The code was tested against eighteen benchmarks, where the models were taken from the ICSBEP *International Handbook of Evaluated Criticality Safety Benchmark Experiments* [7], while the benchmark results were taken from the literature [8]. These benchmarks range from the Godiva bare sphere system to the RA-6 open pool research reactor, comparing the measured kinetic parameters with calculated values using MCNP and OpenMC(TD). The aim of this work is to show an alternative way to obtain nuclear reactor kinetic parameter values using an open source Monte Carlo code.

2. OpenMC Monte Carlo code

The Monte Carlo code OpenMC [6] is a relatively new, open-source code for particle transport. This code is capable of simulating neutron transport in fixed source, k-eigenvalue, and

* Corresponding author. Comisión Chilena de Energía Nuclear, Nueva Bilbao, 12501, Las Condes, Santiago, Chile.
E-mail address: romeroj@uchile.cl (J. Romero-Barrientos).

Table 1
Description of benchmarks studied in this work.

| Case number	Case name	Case description	Benchmark data
1	Godiva	Bare and homogeneous sphere of highly enriched uranium.	k_{eff}, β_{eff}
2	Jezebel-Pu	Bare and homogeneous sphere of plutonium.	k_{eff}, β_{eff}
3	Skidoo	Bare sphere of U-233.	k_{eff}, β_{eff}
4	Topsy	Highly enriched uranium sphere surrounded by a natural uranium reflector.	k_{eff}, β_{eff}
5	Popsy	Plutonium sphere surrounded by a natural uranium reflector.	k_{eff}, β_{eff}
6	Flattop23	U-233 sphere surrounded by a natural uranium reflector.	k_{eff}, β_{eff}
7	BigTen	Intermediate enriched uranium cylindrical core surrounded by a natural uranium reflector.	k_{eff}, β_{eff}
8	ZPR-U9	Cylindrical assembly of uranium metal with a depleted uranium reflector.	k_{eff}, β_{eff}
9	SNEAK-7A	Unmoderated PuO_2/UO_2 core with a depleted uranium reflector.	k_{eff}, β_{eff}
10	SNEAK-7B	Unmoderated PuO_2/UO_2 core with a depleted uranium reflector.	k_{eff}, β_{eff}
11	TCA	Light water moderated low enriched UO_2 core in tank-type critical assembly.	k_{eff}, β_{eff}
12	Stacy-029	Water-reflected cylindrical tank with uranyl nitrate solution.	k_{eff}, α_R
13	Stacy-033	Water-reflected cylindrical tank with uranyl nitrate solution.	k_{eff}, α_R
14	Stacy-046	Water-reflected cylindrical tank with uranyl nitrate solution.	k_{eff}, α_R
15	Stacy-030	Unreflected cylindrical tank with uranyl nitrate solution.	k_{eff}, α_R
16	Stacy-125	Water reflected slabs of enriched uranyl nitrate solution.	k_{eff}, α_R
17	RA-6 (Case 1)	Intermediate enriched uranium open pool research reactor. Water reflected configuration.	k_{eff}
18	RA-6 (Case 2)	Intermediate enriched uranium open pool research reactor. Graphite reflected configuration.	k_{eff}, α_R

Table 2
Results obtained for the effective multiplication factor. k_{eff} was calculated using MCNP6 and OpenMC(TD). Both uncertainties and differences are in pcm.

Case Nº	Case name	k_{eff} exp.	k_{eff} MCNP	k_{eff} OpenMC(TD)	k_{eff} difference (pcm) Exp. - MCNP	k_{eff} difference (pcm) Exp. - OpenMC(TD)	k_{eff} difference (pcm) MCNP - OpenMC(TD)
1	Godiva	1.00000(100)	0.99977(5)	0.99976(5)	23(100)	24(100)	1(7)
2	Jezebel-Pu	1.00000(200)	0.99991(5)	0.99985(5)	9(200)	15(200)	6(6)
3	Skidoo	1.00000(100)	0.99991(5)	0.99991(5)	9(100)	9(100)	0(6)
4	Topsy	1.00100(130)	1.00156(5)	1.00156(6)	−56(130)	−56(130)	0(8)
5	Popsy	1.00000(300)	1.00102(5)	1.00096(6)	−102(300)	−96(300)	6(8)
6	Flattop23	1.00000(140)	0.99880(5)	0.99875(6)	120(140)	125(140)	5(8)
7	BigTen	1.00490(80)	1.00461(5)	1.00462(5)	29(80)	28(80)	−1(6)
8	ZPR-U9	0.99540(240)	0.99625(5)	0.99623(5)	−85(240)	−83(240)	2(6)
9	SNEAK-7A	0.99980(350)	1.00322(5)	1.00310(6)	−342(350)	−330(350)	12(7)
10	SNEAK-7B	1.00010(400)	0.99904(5)	0.99943(5)	106(400)	67(400)	−39(6)
11	TCA	1.00000(200)	0.99999(5)	1.00015(6)	1(200)	−15(200)	−16(7)
12	Stacy-029	0.99990(90)	1.00141(5)	1.00210(5)	−151(90)	−220(90)	−69(6)
13	Stacy-033	0.99990(90)	0.99707(5)	1.00002(5)	283(90)	−12(90)	−295(6)
14	Stacy-046	0.99990(100)	1.00170(5)	1.00226(5)	−180(100)	−236(100)	−56(6)
15	Stacy-030	0.99730(90)	0.99705(5)	0.99824(5)	25(90)	−94(90)	−119(6)
16	Stacy-125	0.99940(140)	1.00498(5)	1.00611(5)	−558(140)	−671(140)	−113(6)
17	RA-6 (Case 1)	1.00160(140)	1.00108(9)	1.00132(10)	−191(250)	28(140)	−24(13)
18	RA-6 (Case 2)	1.00260(250)	1.00451(9)	1.00589(10)	52(140)	−329(250)	−138(13)

Table 3
Results obtained for the effective delayed neutron fraction. Effective delayed neutron fractions, statistical uncertainties and differences are in pcm.

Case Nº	Case Name	β_{eff} Exp.	β_{eff} MCNP	β_{eff} OpenMC(TD)	β_{eff} difference Exp. - MCNP	β_{eff} difference Exp. - OpenMC(TD)	β_{eff} difference MCNP - OpenMC(TD)
1	Godiva	659(10)	660(7)	633(7)	−1(12)	26(12)	27(10)
2	Jezebel-Pu	194(10)	190(4)	181(7)	4(11)	13(12)	9(8)
3	Skidoo	290(10)	297(5)	293(7)	−7(11)	−3(12)	4(9)
4	Topsy	665(13)	686(5)	688(8)	−21(14)	−23(16)	−2(10)
5	Popsy	276(7)	279(5)	280(8)	−3(9)	−4(11)	−1(10)
6	Flattop23	360(9)	360(5)	357(8)	0(10)	3(12)	3(10)
7	BigTen	720(7)	711(7)	696(7)	9(10)	24(10)	15(10)
8	ZPR-U9	725(17)	722(7)	700(7)	3(18)	25(18)	22(10)
9	SNEAK-7A	395(12)	361(5)	319(8)	34(13)	76(14)	42(9)
10	SNEAK-7B	429(13)	411(6)	374(7)	18(14)	55(15)	37(9)
11	TCA	771(7)	765(6)	766(10)	6(9)	5(12)	−1(12)
12	Stacy-029	–	730(6)	713(8)	–	–	17(10)
13	Stacy-033	–	719(6)	718(8)	–	–	1(10)
14	Stacy-046	–	718(6)	709(8)	–	–	9(9)
15	Stacy-030	–	732(6)	736(8)	–	–	−4(10)
16	Stacy-125	–	753(7)	753(8)	–	–	0(10)
17	RA-6 (Case 1)	–	764(11)	746(14)	–	–	18(18)
18	RA-6 (Case 2)	–	741(11)	769(14)	–	–	−28(18)
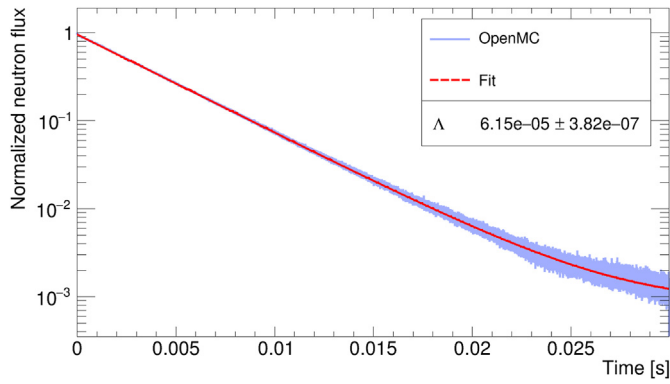
Fig. 1. Time evolution of the normalized neutron flux obtained using OpenMC(TD) for the benchmark Stacy-029. The time evolution of the neutron flux is shown in blue, while the fit obtained is shown in red. Λ value obtained from the fit is also shown. (For interpretation of the references to colour in this figure legend, the reader is referred to the Web version of this article.)

Fig. 2. Time evolution of the normalized neutron flux obtained using OpenMC(TD) for the benchmark RA-6 case 2. The time evolution of the neutron flux is shown in blue, while the fit obtained is shown in red. Λ value obtained from the fit is also shown. (For interpretation of the references to colour in this figure legend, the reader is referred to the Web version of this article.)

subcritical multiplication problems. The code supports both continuous-energy and multigroup cross sections. OpenMC estimates physical quantities, such as neutron flux, through *tallies*; *filters* are used to specify a region of the phase space, for example, scoring neutron flux for a given cell position. The continuous-energy nuclear cross section data follows the HDF5 format [9] and is generated from ACE files produced by NJOY [10]. This code is open source, and its license allows to modify the source code to develop and add new capabilities. An example of this last point is the many number of publications associated to the code, covering topics and developments such as benchmarking [11], coupling and multi-physics [12], geometry and visualization [13], multigroup cross section generation [14], doppler broadening [15], nuclear data [16], parallelism [17], depletion [18] and sensitivity analysis [19].
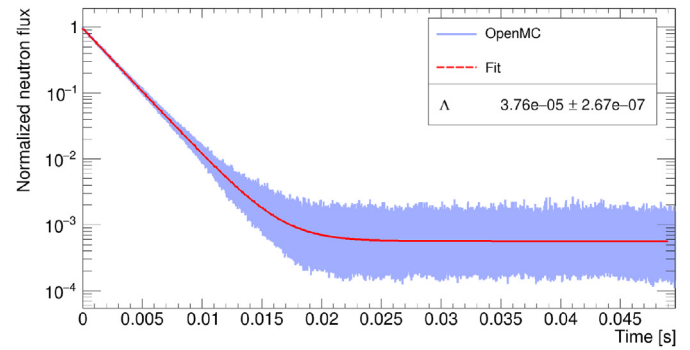
3. Methodology

3.1. Addition of time-dependent capabilities to OpenMC

In a stationary Monte Carlo transport simulation, time is not explicitly present and for the same reason, quantities that change in time cannot be directly obtained. Consequently, the first step to include time explicitly in a Monte Carlo simulation was adding a new label t to the particles, serving as a *clock*, which value was updated using the kinetic energy and the distance traveled by the neutron between any interaction. This time was set to zero $(t = 0)$ at the beginning of the simulation, i.e. when the first particle is emitted from the source, and it was updated while the particle was transported through the geometry of the simulation. After adding the time label to the simulation and in order to account the measured quantities in time, the OpenMC *tallies* were modified and a new *time filter* was included. This filter added the capability to monitor the time evolution of any of the tallies already present in the code. This capability allows to tally, for example, neutron flux as a function of time. The user can define the length and number of the time intervals as desired. This was implemented as the first part of the work developed during the corresponding author's PhD thesis [20], using the version of OpenMC 0.10, written in Fortran. The current version of OpenMC is 0.12.2, written in C++.

3.2. Effective delayed neutron fraction β_{eff}

The effective delayed neutron fraction is defined as the ratio between the adjoint neutron flux and the spectrum weighted number of fissions induced by delayed neutrons and number of fissions induced by all neutrons,

$$\beta_{eff} = \frac{\int \phi^\dagger(\vec{r}, E, \vec{\Omega}) \chi_d(E) \beta \nu(E) \Sigma_f(\vec{r}, E) \phi(\vec{r}, E, \vec{\Omega}) dE d\vec{\Omega} d\vec{r}}{\int \phi^\dagger(\vec{r}, E, \vec{\Omega}) \chi(E) \nu(E) \Sigma_f(\vec{r}, E) \phi(\vec{r}, E, \vec{\Omega}) dE d\vec{\Omega} d\vec{r},} \tag{1}$$

where ϕ is the neutron flux, $\phi^\dagger$ is the adjoint neutron flux, $\vec{r}$ is the neutron position, E is the neutron energy, $\vec{\Omega}$ is the neutron direction, $\chi_d(E)$ the delayed neutron energy spectrum, $\chi(E)$ the fission neutron energy spectrum, β the delayed neutron fraction, $\nu(E)$ is the average number of neutrons released per fission, and Σ_f is the macroscopic fission cross section. MCNP can calculate the effective delayed neutron fraction, Rossi-α and neutron generation time values using the iterated fission probability method, computing adjoint-weighted tallies in criticality calculations [21].

As it can be seen in Eq. (1), formally the adjoint neutron flux is needed to estimate β_{eff}, but in this work, the effective delayed neutron fraction was calculated using the prompt method [22]. This method estimates the value of β_{eff} by:

$$\beta_{eff} \sim 1 - \frac{k_p}{k_{eff}}, \tag{2}$$

where k_{eff} is the effective multiplication factor obtained from a criticality calculation, and k_p is the effective multiplication factor obtained without taking into account the delayed neutrons contribution. With the prompt method the adjoint neutron flux is not needed to calculate β_{eff}. Thus, criticality calculation without delayed neutrons was added as a new capability to OpenMC(TD). This enabled the estimation of β_{eff} by running a criticality calculation for k_{eff} and other for k_p.

3.3. Mean neutron generation time Λ

Another important kinetic parameter to characterize the dynamics of a nuclear reactor is the mean neutron generation time, Λ, defined as

$$\Lambda = \frac{l}{k}, \tag{3}$$

where l is the prompt neutron lifetime and k is the multiplication factor. This means that Λ is the time between the birth of a neutron

Table 4
Results obtained for the prompt generation times. Effective prompt generation times, statistical uncertainties and differences are in seconds and the scaling factor is given in the last column.

Case Number	Case Name	Λ MCNP	Λ OpenMC(TD)	Λ difference MCNP6 - OpenMC(TD)	Scaling Factor
1	Godiva	5.689(8)	5.699(95)	−0.010(100)	$\times 10^{-9}$
2	Jezebel-Pu	2.874(4)	2.879(60)	−0.005(60)	$\times 10^{-9}$
3	Skidoo	2.744(4)	2.760(18)	−0.016(18)	$\times 10^{-9}$
4	Topsy	1.791(4)	1.936(6)	−0.145(7)	$\times 10^{-8}$
5	Popsy	1.323(4)	1.394(8)	−0.071(9)	$\times 10^{-8}$
6	Flattop23	1.258(4)	1.330(7)	−0.073(8)	$\times 10^{-8}$
7	BigTen	6.134(4)	6.338(10)	−0.204(11)	$\times 10^{-8}$
8	ZPR-U9	8.669(12)	8.862(41)	−0.193(43)	$\times 10^{-8}$
9	SNEAK-7A	1.875(4)	1.876(15)	−0.001(16)	$\times 10^{-7}$
10	SNEAK-7B	1.728(3)	1.748(15)	−0.028(15)	$\times 10^{-7}$
11	TCA	3.522(3)	3.742(32)	−0.220(32)	$\times 10^{-5}$
12	Stacy-029	5.962(5)	6.147(38)	−0.185(39)	$\times 10^{-5}$
13	Stacy-033	6.315(6)	6.456(38)	−0.141(38)	$\times 10^{-5}$
14	Stacy-046	6.716(5)	6.993(39)	−0.277(40)	$\times 10^{-5}$
15	Stacy-030	5.853(4)	5.860(32)	−0.007(33)	$\times 10^{-5}$
16	Stacy-125	4.851(4)	5.111(33)	−0.260(33)	$\times 10^{-5}$
17	RA-6 (Case 1)	4.177(10)	4.296(29)	−0.119(31)	$\times 10^{-5}$
18	RA-6 (Case 2)	3.637(7)	3.757(27)	−0.120(28)	$\times 10^{-5}$

Table 5
Results obtained for the measured Rossi-α. Effective delayed neutron fractions, statistical uncertainties and differences are in pcm.

Case Number	Case Name	α_R Exp.	α_R MCNP	α_R OpenMC(TD)	α_R difference Exp. - MCNP	α_R difference Exp. - OpenMC(TD)	α_R difference MCNP - OpenMC(TD)	Scaling Factor
1	Godiva	−1.11(2)	−1.16(2)	−1.11(2)	0.05(3)	0.00(3)	0.05(3)	$\times 10^{6}$
2	Jezebel-Pu	−6.4(1)	−6.60(13)	−6.28(28)	0.20(13)	−0.12(29)	−0.32(31)	$\times 10^{5}$
6	Flattop23	−2.67(5)	−2.86(4)	−2.68(16)	0.19(6)	0.01(17)	−0.18(16)	$\times 10^{5}$
7	BigTen	−1.170(10)	−1.159(12)	−1.098(21)	−0.011(16)	−0.072(23)	0.061(24)	$\times 10^{5}$
12	Stacy-029	−1.227(41)	−1.224(11)	−1.154(14)	−0.003(42)	−0.073(43)	0.070(18)	$\times 10^{2}$
13	Stacy-033	−1.167(39)	−1.138(9)	−1.101(12)	−0.029(40)	−0.066(41)	−0.037(15)	$\times 10^{2}$
14	Stacy-046	−1.062(37)	−1.069(9)	−1.005(15)	0.007(38)	−0.057(40)	−0.064(17)	$\times 10^{2}$
15	Stacy-030	−1.268(29)	−1.251(11)	−1.197(14)	−0.017(31)	−0.071(32)	−0.054(18)	$\times 10^{2}$
16	Stacy-125	−1.528(26)	−1.553(14)	−1.464(17)	0.025(30)	−0.064(31)	−0.089(22)	$\times 10^{2}$
18	RA-6 (Case 2)	−1.808(9)	−1.829(27)	−1.724(27)	0.021(28)	−0.084(28)	−0.105(38)	$\times 10^{2}$

and the subsequent absorption that induces fission. Formally, the neutron generation time is defined in terms of the neutron flux and adjoint neutron flux:

$$\Lambda = \frac{\int \phi^\dagger(\vec{r},E,\vec{\Omega}) \frac{1}{v(E)} \phi(\vec{r},E,\vec{\Omega}) dEd\vec{\Omega}d\vec{r}}{\int \phi^\dagger(\vec{r},E,\vec{\Omega}) \chi(E)\nu(E)\Sigma_f(\vec{r},E)\phi(\vec{r},E,\vec{\Omega}) dEd\vec{\Omega}d\vec{r},} \tag{4}$$

where $v(E)$ is the neutron speed.

In this work the neutron generation time was calculated using the pulsed method [23,24], where a neutron pulse is inserted into a subcritical system and then the neutron population decay is measured. A theoretical approximation used to study this decay is the point kinetics approximation, where the flux is assumed to be a separable function of space and time [25]. Under this assumption the neutron population differential rate, dn/dt, is given by

$$\frac{dn}{dt} = \frac{\rho - \beta_{eff}}{\Lambda} n(t) + \sum_j \lambda_j C_j(t), \tag{5}$$

where ρ is the system reactivity, λ_j and C_j are the decay constant and concentration for the j-th precursor group, respectively. Since the phenomena being studied is the prompt neutron decay, the contribution from delayed neutrons can be neglected,

$$\frac{\partial}{\partial t} n(t) = \frac{\rho - \beta_{eff}}{\Lambda} n(t). \tag{6}$$

The solution to Eq. (6) is given by

$$n(t) = n_0 e^{\alpha t}, \quad \text{with} \quad \alpha = \frac{\rho - \beta_{eff}}{\Lambda} \tag{7}$$

where n_0 is the initial neutron population and α is the decay constant. The expanded time-dependent capabilities added to OpenMC(TD), described in Sec. 3, were used to obtain the decay of the neutron flux as a function of time after placing a neutron source in a subcritical system. The reactivity of the system, ρ, was calculated in a previous criticality run, and β_{eff} was estimated by using the prompt method. Finally, Λ was obtained by fitting Eq. (7) to the neutron population decay curve from the simulation.

4. OpenMC(TD) benchmarks

The modifications added to the OpenMC code were tested using a set of eighteen benchmarks taken from the International Handbook of Evaluated Criticality Safety Benchmark Experiments [7]. Different cases studied in this work includes uranium, plutonium, and U-233 fuel systems, with both thermal and fast neutron energy spectra:

- *Godiva (HEU-MET-FAST-001)*: Bare sphere of highly enriched uranium. The isotopes present in this benchmark are ^{233}U, ^{235}U and ^{238}U.
- *Jezebel-Pu (PU-MET-FAST-001)*: Bare sphere of plutonium. The isotopes present in this benchmark are ^{nat}Ga, ^{239}Pu, ^{240}Pu and ^{241}Pu.
- *Skidoo (U233-MET-FAST-001)*: Bare sphere of uranium, were ^{233}U is at 98%. The isotopes present in this benchmark are ^{233}U, ^{234}U, ^{235}U and ^{238}U.
- *Topsy (HEU-MET-FAST-028)*: Enriched uranium sphere surrounded by a reflector of natural uranium. The isotopes present in this benchmark are ^{234}U, ^{235}U and ^{238}U.
- *Popsy (PU-MET-FAST-006)*: Plutonium sphere surrounded by a reflector of natural uranium. The isotopes present in this benchmark are ^{nat}Ga, ^{239}Pu, ^{240}Pu and ^{241}Pu, ^{234}U, ^{235}U and ^{238}U.
- *Flattop23 (U233-MET-FAST-006)*: Uranium sphere surrounded by a reflector of natural uranium. The isotopes present in this benchmark are ^{233}U, ^{234}U, ^{235}U and ^{238}U.
- *BigTen (IEU-MET-FAST-007)*: Mixed uranium-metal cylindrical core with 10% average ^{235}U enrichment surrounded by a reflector of depleted uranium. The isotopes present in this benchmark are ^{234}U, ^{235}U, ^{236}U, and ^{238}U.
- *ZPR-U9 (IEU-MET-FAST-010)*: Cylindrical assembly of uranium metal with a depleted uranium reflector. The isotopes present in this benchmark are ^{234}U, ^{235}U, ^{236}U, ^{238}U, Ni, Cr, Fe, Si, Mo, Cu, ^{27}Al, C, Mg, ^{1}H, ^{2}H, and ^{19}F.
- *SNEAK-7A, -7B*: Unmoderated PuO$_2$/UO$_2$ with a depleted uranium reflector. The isotopes present in this benchmark are ^{235}U, ^{238}U, ^{239}Pu, ^{240}Pu, ^{241}Pu, ^{242}Pu, Ni, Cr, Fe, Si, Mo, ^{27}Al, C, Mg, and O.
- *TCA*: Light water, moderated and low-enriched UO$_2$ core in a tank-tpe critical assembly. The isotopes present in this benchmark are ^{234}U, ^{235}U, ^{238}U, ^{1}H, ^{16}O, and ^{27}Al.
- *Stacy-029, -033, -046 (LEU-SOL-THERM-004)*: Water-reflected cylindrical tank with uranyl-nitrate solution at 10% enrichment. The isotopes present in this benchmark are ^{234}U, ^{235}U, ^{238}U, ^{1}H, ^{14}N, and ^{16}O.
- *Stacy-030 (LEU-SOL-THERM-007)*: Water-reflected cylindrical tank with uranyl-nitrate solution at 10% enrichment. The isotopes present in this benchmark are ^{234}U, ^{235}U, ^{238}U, ^{1}H, ^{14}N, and ^{16}O.
- *Stacy-125 (LEU-SOL-THERM-016)*: Water-reflected slabs of 10% enriched uranyl nitrate solution. The isotopes present in this benchmark are ^{234}U, ^{235}U, ^{236}U, ^{238}U, ^{1}H, ^{16}O, ^{17}O, C, Si, Ni, Fe, and Cr.
- *RA-6 (IEU-COMP-THERM-014)*: Open pool research reactor, fuel elements are MTR-type with 19.7% enrichment. Two configurations were studied, which are detailed in Sec. 4.1

The systems described above are summarized in Table 1.

4.1. Description of the RA-6 reactor

The RA-6 (spanish acronym for Argentina Reactor, Number 6) is an open pool research reactor with a nominal power of 3 MW, located in the Bariloche Atomic Center, San Carlos de Bariloche, Río Negro, Argentina. The core of the reactor is made up of an array of flat plate MTR-type fuel elements with 20% enriched uranium located inside a stainless steel tank filled with demineralized water that acts as a coolant, moderator, reflector and shielding in the axial direction. Reactivity is controlled by four Ag−In−Cd plates. The fuel elements were modeled explicitly, including the cadmium wires, water gaps, guides and nozzles. The model also included the supporting grid for the core and BNCT filter. Two configurations were studied: Case 1 corresponds to a water reflected configuration and

it was the first critical configuration included in ICSBEP. Case 2 corresponds to a graphite reflected configuration [26].

5. Results

5.1. Effective multiplication factor

Results obtained for the effective multiplication factor calculated with MCNP and OpenMC(TD) are shown in Table 2, along with the experimental value when available, the difference between experimental and OpenMC(TD) calculated values, and the difference between MCNP and OpenMC(TD) calculated values. These criticality calculations were run using 100 inactive and 2000 active batches of 200000 source neutrons, with the ENDF/B-VII.1 nuclear cross section libraries [27]. By examining Table 2 it can be seen that uncertainties obtained for MCNP and OpenMC(TD) were less than 5 and 6 pcm, respectively, except for the RA-6 cases, where the simulation uncertainties were 9 and 10 pcm. k_{eff} values obtained from both simulations are within benchmark uncertainties for 13 of the 18 cases and the differences between calculated values and benchmark uncertainties were less than 0.3%.

5.2. Effective delayed neutron fraction

Results obtained for the effective delayed neutron fraction calculated with MCNP and OpenMC(TD) are shown in Table 3, along with the experimental value when available, the difference between experimental and OpenMC(TD) calculated values, and the difference between MCNP and OpenMC(TD) calculated values. MCNP estimated β_{eff} with adjoint-weighted tallies using the iterated fission probability method. OpenMC(TD) estimated β_{eff} using the prompt method and the k_p criticality calculations to compute β_{eff} were run using 100 inactive and 2000 active batches of 200000 source neutrons. All of these calculations used ENDF/B-VII.1 nuclear cross section libraries.

By examining Table 3 it can be seen that differences between OpenMC(TD) calculated and benchmark values were less than 26 pcm, except for SNEAK-7A (76 pcm) and SNEAK-7B (55 pcm). For MCNP differences between calculated and benchmark values were less than 34 pcm. β_{eff} values obtained from OpenMC(TD) are within benchmark uncertainties for 4 of the 12 cases. For Stacy-029, Stacy-033, Stacy-046, Stacy-030, Stacy-125 and both RA-6 cases there are no β_{eff} experimental measurements available.

5.3. Mean neutron generation time

Neutron flux as a function of time calculated using OpenMC(TD) was obtained for the 18 benchmark cases shown in Table 1. These fixed-source calculations were run using 100 batches of 200000 source neutrons. As an example of results obtained, the neutron flux as a function of time for the Stacy-030 and RA-6 cases are shown in Fig. 1 and Fig. 2, respectively.

Results for the calculated mean neutron generation time obtained with MCNP and OpenMC(TD) are shown in Table 4. By examining results obtained it can be seen that the difference between MCNP and OpenMC(TD) are less than 7%, except for Topsy, where the difference is of 8.1%.

In systems from Table 1, Λ is not reported explicitly, nevertheless, $\alpha_R = \beta_{eff}/\Lambda$ [4] is reported for some of the benchmarks and its results are compared to simulations in Table 5. It can be seen that for OpenMC(TD) the difference between benchmark and calculated values is less than 6.56%, while for MCNP this difference is less than 4.31% except for Flattop23 case where it is 6.64%.

6. Summary and conclusions

This work presented the methodology developed to include time dependence for the open source Monte Carlo code OpenMC. The modified code, OpenMC(TD), was used to calculate the effective delayed neutron fraction β_{eff} using the prompt method. The mean neutron generation time Λ was estimated by scoring the decay of the neutron population after using the pulsed method. MCNP estimates β_{eff}, Λ, and α_R using adjoint-weighted tallies in a criticality calculation. In OpenMC, β_{eff} was obtained using the prompt method approximation, while Λ and α_R were calculated using OpenMC(TD) new time-dependence capabilities, through a fit, as it was shown in Figs. 1 and 2. It is important to notice that the pulsed method is an approximation that requires a slightly subcritical system to observe the decay of the neutron flux in a fixed-source calculation.

For the effective delayed neutron fraction, it can be seen that differences between OpenMC(TD) calculated and benchmark values were less than 26 pcm, except for two cases, SNEAK-7A (76 pcm) and SNEAK-7B (55 pcm). In the case of MCNP, differences between calculated and benchmark values were less than 34 pcm. β_{eff} values obtained from OpenMC(TD) are within benchmark uncertainties for 4 of the 12 cases. For the neutron generation time, the difference between MCNP and OpenMC(TD) are less than 7%, except for Topsy, where the difference is of 8.1%. For Rossi-α, the difference between benchmark and OpenMC(TD) calculated values is less than 6.56%, while for MCNP this difference is less than 4.31% except for Flattop23 case where it is 6.64%.

Nevertheless, implementation of time dependence in the open source code OpenMC lays the groundwork for the development of studies for the inclusion of β-delayed neutron emission from individual precursors. This was the main objective of the corresponding author's PhD thesis [20]. Contribution of these developments to the main branch of OpenMC shown in this work are expected to be implemented in the near future [28].

Declaration of competing interest

The authors declare that they have no known competing financial interests or personal relationships that could have appeared to influence the work reported in this paper.

Acknowledgments

References

[1] T. Goorley, M. James, T. Booth, F. Brown, J. Bull, L.J. Cox, J. Durkee, J. Elson, M. Fensin, R.A. Forster, J. Hendricks, H.G. Hughes, R. Johns, B. Kiedrowski, R. Martz, S. Mashnik, G. McKinney, D. Pelowitz, R. Prael, J. Sweezy, L. Waters, T. Wilcox, T. Zukaitis, Initial MCNP6 release overview, Nucl. Technol. 180 (3) (2012) 298–315, https://doi.org/10.13182/NT11-135.

[2] H. J. Shim, B.-S. Han, J.-S. Jung, H. J. Park, C.-H. Kim, McCARD: Monte Carlo code for advanced reactor design and analysis, Nucl. Eng.Technol. 44. doi:10.5516/NET.01.2012.503.

[3] J. Leppänen, M. Pusa, T. Viitanen, V. Valtavirta, T. Kaltiaisenaho, The serpent Monte Carlo code: status, development and applications in 2013, Ann. Nucl. Energy 82 (2015) 142–150, https://doi.org/10.1016/j.anucene.2014.08.024.

[4] R. D. Mosteller, B. C. Kiedrowski, The Rossi Alpha Validation Suite for MCNP, LA-UR-11-04409 Los Alamos National Laboratory.

[5] A.G. Mylonakis, M. Varvayanni, D. Grigoriadis, N. Catsaros, Developing and investigating a pure monte-carlo module for transient neutron transport analysis, Ann. Nucl. Energy 104 (2017) 103–112, https://doi.org/10.1016/j.anucene.2016.12.039.

[6] P.K. Romano, N.E. Horelik, B.R. Herman, A.G. Nelson, B. Forget, K. Smith, OpenMC: a state-of-the-art Monte Carlo code for research and development, Ann. Nucl. Energy 82 (2015) 90–97, https://doi.org/10.1016/j.anucene.2014.07.048. Joint International Conference on Supercomputing in Nuclear Applications and Monte Carlo 2013.

[7] J.B. Briggs, L. Scott, A. Nouri, The international criticality safety benchmark evaluation project, Nucl. Sci. Eng. 145 (1) (2003) 1–10, https://doi.org/10.13182/NSE03-14.

[8] J. Leppänen, M. Aufiero, E. Fridman, R. Rachamin, S. van der Marck, Calculation of effective point kinetics parameters in the Serpent 2 Monte Carlo code, Ann. Nucl. Energy 65 (2014) 272–279, https://doi.org/10.1016/j.anucene.2013.10.032.

[9] S. Koranne, Hierarchical Data Format 5 : HDF5, Springer US, Boston, MA, 2011, pp. 191–200, https://doi.org/10.1007/978-1-4419-7719-9_10.

[10] R. Macfarlane, D. W. Muir, R. M. Boicourt, A. C. Kahler, III, J. L. Conlin, The NJOY Nuclear Data Processing System, Version 2016, Technical Report Los Alamos National Laboratory (TRN: US1701456). doi:10.2172/1338791.

[11] K.S. Chaudri, S.M. Mirza, Burnup dependent Monte Carlo neutron physics calculations of IAEA MTR benchmark, Prog. Nucl. Energy 81 (2015) 43–52, https://doi.org/10.1016/j.pnucene.2014.12.018.

[12] J. Chen, L. Cao, C. Zhao, Z. Liu, Development of Subchannel Code SUBSC for High-Fidelity Multi-Physics Coupling Application, Energy Procedia, vol. 127, international Youth Nuclear Congress 2016, Hangzhou, China, 2017, pp. 264–274, https://doi.org/10.1016/j.egypro.2017.08.121. IYNC2016, 24-30 July 2016.

[13] J.-Y. Li, L. Gu, H.-S. Xu, N. Korepanova, R. Yu, Y.-L. Zhu, C.-P. Qin, CAD modeling study on FLUKA and OpenMC for accelerator driven system simulation, Ann. Nucl. Energy 114 (2018) 329–341, https://doi.org/10.1016/j.anucene.2017.12.050.

[14] I. Variansyah, B.R. Betzler, W.R. Martin, Multigroup constant calculation with static α-eigenvalue Monte Carlo for time-dependent neutron transport simulations, Nucl. Sci. Eng. 194 (11) (2020) 1025–1043, https://doi.org/10.1080/00295639.2020.1743578.

[15] J.A. Walsh, B. Forget, K.S. Smith, F.B. Brown, On-the-fly Doppler broadening of unresolved resonance region cross sections, Prog. Nucl. Energy 101 (2017) 444–460, https://doi.org/10.1016/j.pnucene.2017.05.032, special Issue on the Physics of Reactors International Conference PHYSOR 2016: Unifying Theory and Experiments in the 21st Century.

[16] J.A. Walsh, P.K. Romano, B. Forget, K.S. Smith, Optimizations of the energy grid search algorithm in continuous-energy Monte Carlo particle transport codes, Comput. Phys. Commun. 196 (2015) 134–142, https://doi.org/10.1016/j.cpc.2015.05.025.

[17] P.K. Romano, A.R. Siegel, B. Forget, K. Smith, Data decomposition of Monte Carlo particle transport simulations via tally servers, J. Comput. Phys. 252 (2013) 20–36, https://doi.org/10.1016/j.jcp.2013.06.011.

[18] B. Zhang, X. Yuan, Y. Zhang, H. Tang, L. Cao, Development of a versatile depletion code AMAC, Ann. Nucl. Energy 143 (2020) 107446, https://doi.org/10.1016/j.anucene.2020.107446.

[19] X. Peng, J. Liang, B. Forget, K. Smith, Calculation of adjoint-weighted reactor kinetics parameters in OpenMC, Ann. Nucl. Energy 128 (2019) 231–235, https://doi.org/10.1016/j.anucene.2019.01.007.

[20] J. Romero-Barrientos, Time-dependent Monte Carlo in Fissile Systems with Beta-Delayed Neutron Precursors, Ph.D. thesis, 2021. arXiv:2101.09338.

[21] B. C. Kiedrowski, Theory, interface, verification, validation, and performance of the adjoint-weighted point reactor kinetics parameter calculations in MCNP, LA-UR-10-01700 Los Alamos National Laboratory.

[22] R.K. Meulekamp, S.C. van der Marck, Calculating the effective delayed neutron fraction with Monte Carlo, Nucl. Sci. Eng. 152 (2) (2006) 142–148, https://doi.org/10.13182/NSE03-107.

[23] B.E. Simmons, J.S. King, A pulsed neutron technique for reactivity determination, Nucl. Sci. Eng. 3 (5) (1958) 595–608, https://doi.org/10.13182/NSE3-595-608.

[24] L. Snoj, A. Kavčič, G. Žerovnik, M. Ravnik, Calculation of kinetic parameters for mixed TRIGA cores with Monte Carlo, Ann. Nucl. Energy 37 (2) (2010) 223–229, https://doi.org/10.1016/j.anucene.2009.10.020.

[25] G.I. Bell, S. Glasstone, Nuclear Reactor Theory, Van Nostrand Reinhold, 1970.

[26] S. Bazzana, Desarrollo, análisis y evaluación de experimentos neutrónicos en el RA-6, Master's thesis, Instituto Balseiro, Universidad Nacional de Cuyo, Comisión Nacional de Energía Atómica, Argentina, San Carlos de Bariloche, Argentina, 2012.

[27] M. Chadwick, M. Herman, P. Obložinský, M. Dunn, Y. Danon, A. Kahler, D. Smith, B. Pritychenko, G. Arbanas, R. Arcilla, R. Brewer, D. Brown, R. Capote, A. Carlson, Y. Cho, H. Derrien, K. Guber, G. Hale, S. Hoblit, S. Holloway, T. Johnson, T. Kawano, B. Kiedrowski, H. Kim, S. Kunieda, N. Larson, L. Leal, J. Lestone, R. Little, E. McCutchan, R. MacFarlane, M. MacInnes, C. Mattoon, R. McKnight, S. Mughabghab, G. Nobre, G. Palmiotti, A. Palumbo, M. Pigni, V. Pronyaev, R. Sayer, A. Sonzogni, N. Summers, P. Talou, I. Thompson, A. Trkov, R. Vogt, S. van der Marck, A. Wallner, M. White, D. Wiarda, P. Young, ENDF/B-VII.1 nuclear data for science and technology: cross sections, covariances, fission product yields and decay data, Nucl. Data Sheets 112 (12) (2011) 2887–2996, https://doi.org/10.1016/j.nds.2011.11.002, special Issue on ENDF/B-VII.1 Library.

[28] P.K. Romano, Private Communication, February 2021.